



HAL
open science

Impact of RF stress on different topologies of 100 nm X-band robust GaN LNA

B. Pinault, Jean-Guy Tartarin, D. Saugnon, R. Leblanc

► **To cite this version:**

B. Pinault, Jean-Guy Tartarin, D. Saugnon, R. Leblanc. Impact of RF stress on different topologies of 100 nm X-band robust GaN LNA. *Microelectronics Reliability*, 2023, Special issue of 34th European Symposium on Reliability of Electron Devices, Failure Physics and Analysis, ESREF 2023, 150, pp.115126. 10.1016/j.microrel.2023.115126 . hal-04493506

HAL Id: hal-04493506

<https://hal.science/hal-04493506>

Submitted on 7 Mar 2024

HAL is a multi-disciplinary open access archive for the deposit and dissemination of scientific research documents, whether they are published or not. The documents may come from teaching and research institutions in France or abroad, or from public or private research centers.

L'archive ouverte pluridisciplinaire **HAL**, est destinée au dépôt et à la diffusion de documents scientifiques de niveau recherche, publiés ou non, émanant des établissements d'enseignement et de recherche français ou étrangers, des laboratoires publics ou privés.



Distributed under a Creative Commons Attribution - NoDerivatives 4.0 International License

Impact of RF stress on different topologies of 100 nm X-band Robust GaN LNA

B. Pinault^{a,b}, J.G. Tartarin^{a,b}, D. Saugnon^a, , R. Leblanc^c

^a *Laboratoire d'analyse et d'architecture des systèmes (LAAS-CNRS), Toulouse, France*

^b *Paul Sabatier University, University of Toulouse, Toulouse, France*

^c *OMMIC, Limeil-Brévannes, France*

Abstract

In this article, we study the robustness of 3 versions of a single stage LNA configured according to different modes of detectivity or robustness against electromagnetic jamming signals. Four successive sequences of RF step stress at 10 GHz are applied to each of the 3 LNAs under study. These robust MMIC LNAs have been designed using the D01GH GaN process from OMMIC technology, to switch from a nominal low noise mode to a high linearity mode. This DC-bias switch allows to increase the power input 1dB compression point by 8 dB. This study focuses on the robustness of these LNAs (LNA_{#A} for agile) when they operate under nominal low-noise mode (featuring lower IP_{1dB}) or under nominal high-linearity mode (at the price of a degraded noise figure NF₅₀). This original LNA_{#A} is compared to a robust conventional design using a larger sized device (LNA_{#R} for robust). The step-stresses are operated at 10 GHz, which is the center frequency band of these LNAs. All modes of operation are shown to exhibit fairly reproducible step stress plots, although thermal or nonlinear effects can be differentiated between low-noise and high-linearity operating conditions, and compared with the robust design LNA_{#R}. We demonstrate the relevance of an alternative approach to conventional LNA circuit design strategies in order to achieve natural electronic protection, without a limiter placed before the LNA_{#A} or LNA_{#R} or without turning-off the DC-biasing: this protection option benefits from maintaining the LNA in an operational detection situation for longer when the incident input signal increases, without any degradation in electrical performance (DC and RF) or noise (NF₅₀), even after many sequences of RF step stress.

Introduction

Due to their intrinsic properties, GaN LNAs offer interesting solutions for applications requiring both high detectivity and robustness to EM aggressions. It allows a new definition of receivers as they can also integrate the RF filter and they can withstand higher temperatures than their GaAs counterparts. They are therefore excellent candidates for Radar and Telecom applications. The ability of a system to withstand high levels of RF power is assessed by its ability to remain operational during an eventual aggression but also to return to a nominal operating mode after a stress period. In order to exploit the characteristics of Gallium Nitride to the fullest, we have designed an LNA capable of being self-reconfigured at two different quiescent points, allowing to combine a low noise figure (NF₅₀) and a high 1dB compression point at the input of the device (IP_{1dB}). Then the same LNA_{#A}, depicted on Figure 1, is able to operate under a nominal low noise mode (NF₅₀=0.95 dB / IP_{1dB}=4 dBm), and under a strongly linear mode

(NF₅₀=1.3 dB / IP_{1dB}=13 dBm), which ensures the increase of the compression point of the device, while maintaining quasi-stable S parameters [1]. This is made possible by designing an ad hoc MMIC circuit topology capable of supporting DC bias reconfiguration, without changing the small-signal electrical performance. The difficulty to design such a reconfigurable LNA consists in maintaining the unconditional stability for each biasing mode, but also for the DC path from a mode to another one. The circuit must also keep its [S] parameters unchanged according to these operating modes. In this study, in order to simplify the cross-interpretation of electrical trends, a single-stage LNA_{#A} is designed, based on an AlGaIn/GaN HEMT with 6 gate fingers of 50 μm individual gate width. This LNA presents a small-signal gain (S₂₁) of more than 10 dB and an input/output matching better than -9 dB over the X-band for the two selected quiescent points. The objective of this paper is to compare the performance and the evolution of important figures of merit of the stability against RF signal jamming of these MMIC

* Corresponding author. bpinault@laas.fr

LNA_{#A}: the drain current I_{DS} , the gate current I_{GS} , the dynamic HF gain S_{21} and output power P_{out} are tracked under the application of a sequence of four successive 10 GHz RF step-stresses [2]. One LNA_{#A-LN} is stressed when biased in its low-noise mode (test 1, at $[V_{DS}=6V / I_{DS}=30mA]$), while another LNA_{#A-HL} is stressed when biased in its high-linearity mode (test 2, at $[V_{DS}=12V / I_{DS}=75mA]$).

A robust design LNA_{#R} ($V_{DS}=12.9V / I_{DS}=45mA$) is also designed (Figure 2), based on an AlGaIn/GaN HEMT with 8 gate fingers of 50 μm individual gate width, as proposed by [2]. It is used to make a comparison between two robust strategies for GaN based receivers. Test 3 corresponds to the RF stress sequence associated to LNA_{#R}.

3 LNAs (two LNA_{#A} and one LNA_{#R}) are submitted to the stress sequences as described in Figure 3. All the measurements have been performed on probe station: a picture of the experimental setup is given in Figure 4. During the stress sequence, the output RF power P_{out} , the DC drain current I_{DS} and gate leakage current I_{GS} are tracked during the step stresses. Noise figure measurement NF50 and [S] parameters are performed before and after 20 dBm stress (sequence #1) and after 30 dBm stress (sequence #2). These measurements, taken during and after the stress, make it possible to assess the interest of the selected approach with regard to the robustness of the circuits [3].

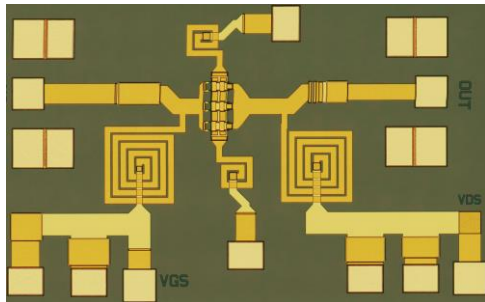


Figure 1: Single-stage reconfigurable – agile MMIC LNA_{#A} (next used under the 2-modes LNA_{#A-LN} -low noise and LNA_{#A-HL}-high-linearity) and b) robust LNA_{#R}. The GaN MMIC technology is D01GH from OMMIC.

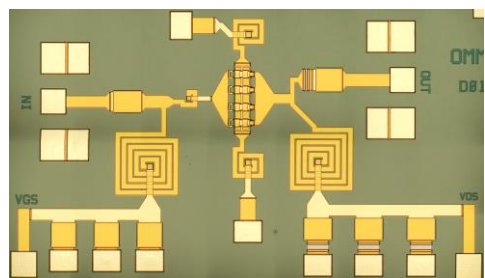


Figure 2: Single-stage robust LNA_{#R}. with a 100nm gate length- from OMMIC technology.

I - RF stress sequences on reconfigurable LNA_{#A} with the robust design LNA_{#R}

I-1 Testing procedure

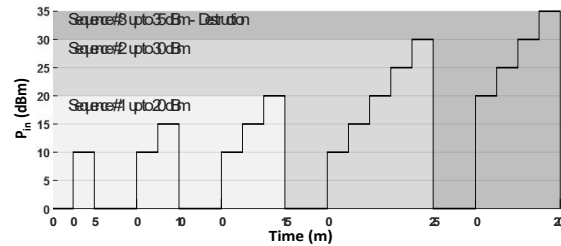


Figure 3: 10 GHz RF stress sequence, with recovery periods. Each LNA is submitted to 3 successive sequences (sequence#1, sequence#2 and sequence#3-destructive) Takeover measurements are performed before stress, and after sequence#1, sequence#2 (sequence#3 is destructive).

The stress test procedure consists in controlling an RF power synthesizer to perform a step-stress starting from 10 dBm, and then incrementing the power by 5 dB step every 5 minutes. Three successive sequences are used for each LNA (namely LNA_{#A-LN} / LNA_{#A-HL} and LNA_{#R}). The different elements of the experimental bench, as well as its calibration are accounted for to determine the effective input and output powers at the LNA's terminals. The procedure is performed on three LNAs: the two first agile LNA_{#A} operate in low noise configuration (LNA_{#A-LN}, test 1) and high linearity mode (LNA_{#A-HL} test 2), while the third LNA_{#R} keeps its biasing constant (LNA_{#R} test 3) [4]. The duration of each step-stress is chosen to be longer than that applied to radar systems on board fighter aircraft. The RF dynamic electrical parameters (P_{out} , dynamic gain defined as $P_{out-dBm} - P_{in-dBm}$) and static (I_{DS} , I_{GS}) are plotted versus the input RF power P_{in} at 10 GHz.

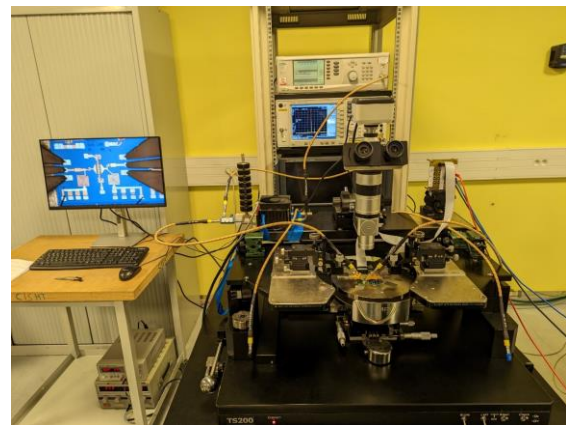


Figure 4: experimental workbench for the RF step-stress at 10 GHz, and takeover measurements. Measurements are performed on probe station TS200 from MPI, with power RF probes. The RF synthesizer associated to a power

amplifier delivers the incident power up to 38 dBm, and a coupler/attenuator is connected to a spectrum analyzer for S_{11} measurement under non-linear RF signal. The output power is measured with the Keysight U8487A power sensor. Takeover measurements are performed with the PNA-X series 5244b from keysight with option 029 for HF noise measurements.

I-2 Electrical measurements during stress

We can see on Figure 5 that LNA_{#R} achieve a higher output saturated power which is due to the fact that the active component inside this LNA is larger. From Figure 5, the linear P_{out} vs P_{in} plot shows almost the same linear gain (S_{21}), while the power compression occurs at different P_{in} level as expected for the different circuit versions. As this study deals with a single-stage amplifier, and as the gain is the same for all of the three LNAs, the output power compression point can be considered as a figure of merit for the compression of the single-tone 10 GHz signal. However, as the LNA aggression occurs at its input, only I_{P1dB} or P_{in} are discussed as the relevant metrics to be considered.

As mentioned previously, each LNA is subjected to a series of 3 RF-stress sequences at increasing RF_{max} power levels. Note that no degradation appears on the plots for input RF signal up to 20 dBm (sequence #1) and also 30dBm (sequence #2). The LNAs are destroyed for incident RF input power between 30 dBm and 35dBm (sequence #3).

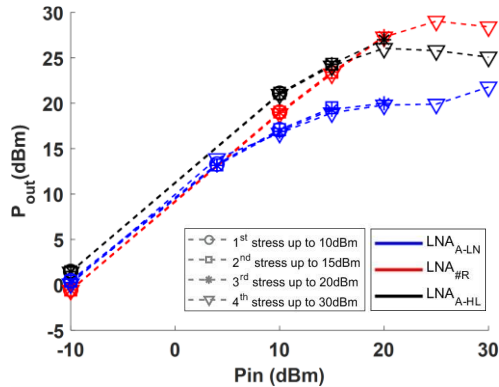


Figure 5: plots of output power versus input power for agile LNA_{#A} (low-noise DC configuration LNA_{#A-LN} and high-linearity DC configuration LNA_{#A-HF}), and robust design LNA_{#R}, at 10 GHz RF stress. The three stress sequences are plotted, according to the testing procedure as described in Figure 3.

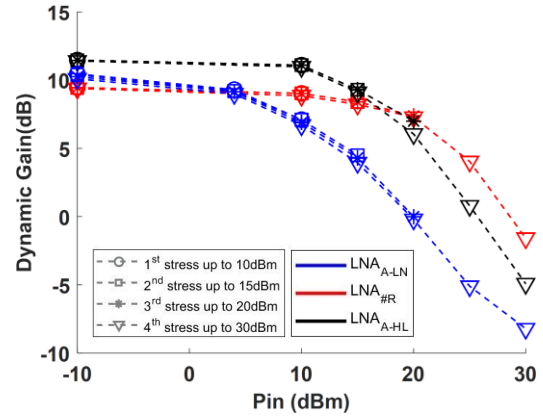


Figure 6: plots of dynamic gain versus input power for agile LNA_{#A} (low-noise DC configuration LNA_{#A-LN} and high-linearity DC configuration LNA_{#A-HF}), and robust design LNA_{#R}, at 10 GHz RF stress.

LNA_{#A-LN} power compression appears at $P_{in}=4$ dBm, and it increases up to $P_{in}=13$ dBm when reconfiguring the DC-biasing as for LNA_{#A-HL}. On its side, LNA_{#R} power compression occurs at $P_{in}=16$ dBm, as a larger device is used to withstand more elevated RF magnitude over its load cycle. Figure 6 is another representation of Figure 5, as the dynamic gain (in dB) is defined as $P_{out}(dBm)-P_{in}(dBm)$ of the signals at 10 GHz. The power range where the gain is constant (i.e. the small-signal gain S_{21}) is clearly evidenced for each of the three LNAs. We have to keep in mind that in a real situation (operational receiver), LNA_{#A} will be initially set at LNA_{#A-LN} when the electromagnetic aggression keeps below a threshold level (that can be set according to the desired level), and self-reconfigured to LNA_{#A-HL} when an elevated RF signal is detected. This proof of concept has been performed for a 2-stage LNA from the same run [5]. LNA_{#R} still operates at the same DC-biasing condition, providing a better I_{P1dB} than for LNA_{#A-HL}, but at the price of a 0.2 dB degradation of the 50 Ω noise figure (NF_{50}) than for LNA_{#A-LN}, as presented in section I.3. DC quiescent conditions are plotted versus the RF input power (Figure 7 and Figure 8), also for 3 stress sequences as described in Figure 3.

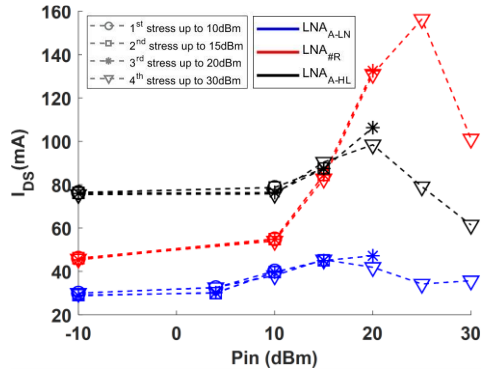


Figure 7: plots of DC-drain current versus input power for agile LNA_{#A} (low-noise DC configuration LNA_{#A-LN} and high-linearity DC configuration LNA_{#A-HL}), and robust design LNA_{#R}, at 10 GHz RF stress. The three stress sequences are plotted, according to the testing procedure as described in Figure 3.

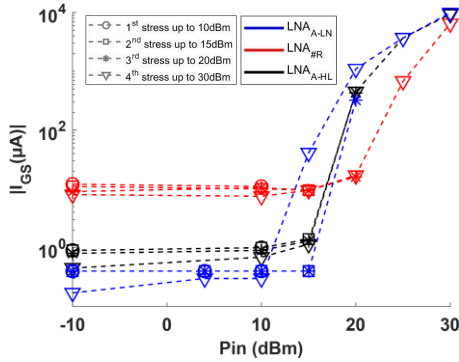


Figure 8: plots of DC-gate leakage current versus input power for agile LNA_{#A} (low-noise DC configuration LNA_{#A-LN} and high-linearity DC configuration LNA_{#A-HL}), and robust design LNA_{#R}, at 10 GHz RF stress.

RF power induced non-linear effects are visible on Figure 7, but surprisingly in a lesser extend for LNA_{#A} (LN or HL configuration). However, the change in DC- I_{DS} corroborates the I_{P1dB} level. The variation on I_{GS} leakage current appears for more elevated input RF power. The maximum I_{GS} level induced by the stress reaches $I_{GSmax}=10$ mA for each three LNAs, even if the increase trends are not similar between the three LNAs under study prior to this critical level at $P_{in}=30$ dBm (or 35 dBm at destruction). This critical leakage current around 10 mA of gate width has already been observed by the authors on different GaN technologies featuring gate length of 100 nm or also 150 nm (RF or DC step stressed devices and circuits): the study is still on-going to make it clear the I_{GS} contribution to the stress.

II – Electrical and HF Noise measurements before stress and after sequence#1 and sequence#2

This section provides the initial measurement (before

the RF stress sequence), and takeover measurements after sequence #1 and after sequence #2. Sequence #3 leads to the destruction of all single-stage LNAs (which prevents any post- measurement)

II-1 [S] parameters measurement before stress and after sequence #1 and sequence #2.

A plot of S_{21} (small-signal gain), S_{11} and S_{22} (resp. input and output reflexion coefficient) versus the RF stress sequences in Figure 9 and Figure 10 (“o” is the initial measurement). The S_{21} gain for robust design remains constant during sequence #1 and sequence #2, as for the high linearity mode LNA_{#A-HL}, whereas the low-noise mode LNA_{#A-LN} degrades by 1dB after sequence #1 and by 2dB after sequence #2. S_{11} and S_{22} parameters remains almost constant and below -10 dB (which is the design criterion to match the accesses of our LNAs), except for LNA_{#A-LN} which degrades by 1dB after sequence #1 and sequence #2.

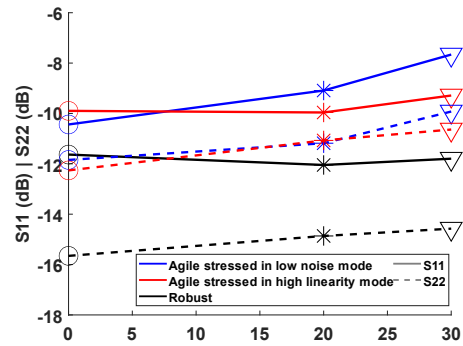


Figure 9: [S] parameters measurement at 10 GHz versus input stress RF level. Reflexion coefficients S_{11} and S_{22} for agile LNA_{#A} (LNA_{#A-LN} and LNA_{#A-HL}), and robust design LNA_{#R}.

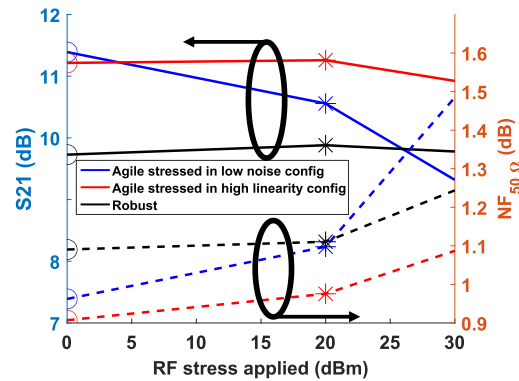


Figure 10: Noise figure and small signal Gain measurement at 10 GHz versus input stress RF level for agile LNA_{#A} (LNA_{#A-LN} and LNA_{#A-HL}), and robust design LNA_{#R}.

II-2 Noise Figure measurement (NF50) before stress and after sequence#1 and sequence#2.

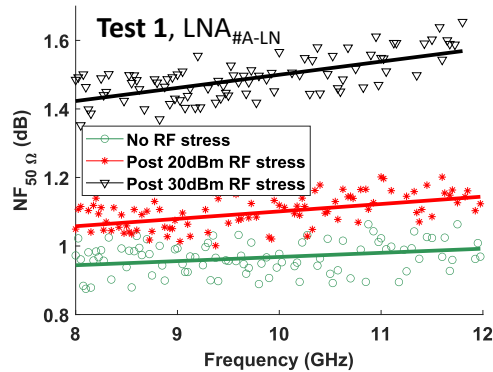


Figure 11: 50 ohms Noise Figure measurement (NF50) from 8 GHz to 12 GHz (40% bandwidth) at t_0 initial state, after sequence #1 ($P_{in}=20$ dBm) and after sequence #2 ($P_{in}=30$ dBm). Test 1 is on LNA_{#A-LN}.

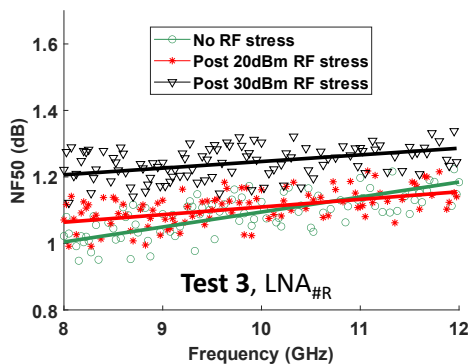


Figure 12: 50 ohms Noise Figure measurement (NF50) from 8 GHz to 12 GHz (40% bandwidth) at t_0 initial state, after sequence #1 ($P_{in}=20$ dBm) and after sequence #2 ($P_{in}=30$ dBm). Test 3 is on LNA_{#R}.

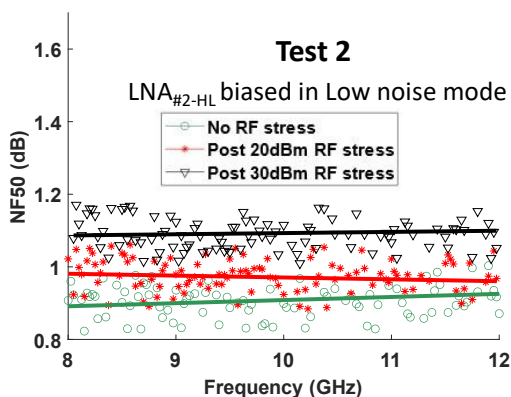


Figure 13: 50 ohms Noise Figure measurement (NF50) from 8 GHz to 12 GHz (40% bandwidth) at t_0 initial state, after sequence #1 ($P_{in}=20$ dBm) and after sequence #2 ($P_{in}=30$ dBm). Test 2 is on LNA_{#A-HL} biased under Low Noise mode for this measurement.

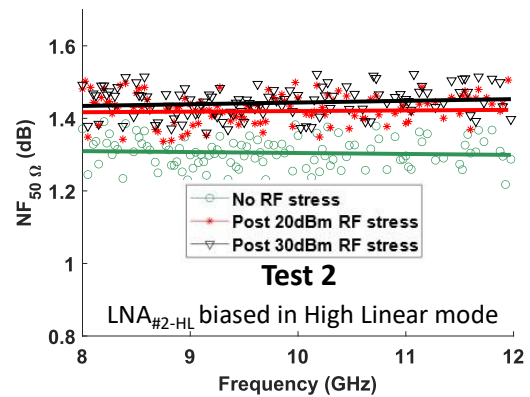


Figure 14: 50 ohms Noise Figure measurement (NF50) from 8 GHz to 12 GHz (40% bandwidth) at t_0 initial state, after sequence #1 ($P_{in}=20$ dBm) and after sequence #2 ($P_{in}=30$ dBm). Test 2 is on LNA_{#A-HL} biased under High Linearity mode for this measurement.

Noise measurement under 50 ohms is performed with the PNA-X series 5244B from Keysight, option 029 (low noise measurement).

- From Figure 11, it is obvious that NF₅₀ of test 1 on LNA_{#A-LN} degrades by 0.1dB and 0.5dB after RF stress of 20dBm (sequence #1) and 30dBm (sequence#2) respectively. As can be seen in Figure 10, a part of this degradation can be directly correlated with the decrease of the device gain.

- The robust design of test 2 (LNA_{#R}) is stable after sequence#1 (Figure 12), and only degrades by 0.2 dB after sequence #2. However, the initial NF₅₀ is not constant over the 8-12GHz bandwidth at t_0 , and is 0.15 dB higher than for LNA_{#A-LN}.

- Test 3 on LNA_{#A-HL} can be measured under low-noise biasing condition (i.e. when coming back to a situation without electromagnetic aggression) or high-linearity condition, respectively with NF₅₀ as depicted in figure 13 and Figure 14. Under both biasing conditions, NF₅₀ degrades by only 0.1dB and 0.2 dB after sequence #1 and sequence #2 respectively, still providing state of the art NF₅₀ in X-band (Figure 13).

II-2 Discussion on SOA.

This last section concerns the evolution of the dissipated power in the active devices (defined as $P_{DC-natural} - [P_{out-natural} - P_{in-natural}]$), regarding the LNA design and biasing, and for different sequences of stress, as depicted in Figure 15. As expected, LNA_{#A-LN} is biased near the pinch-off zone of the transistor, where the transconductance gain g_m is almost at its maximum and the drain current low to get an optimized minimum noise figure NF_{min} . The low dissipated power ensures small electrical and thermal stresses for the LNA, whereas these later are

more pronounced for the version of the same LNA_{#A} biased in high linearity mode (LNA_{#A-HL}). This DC-biasing condition makes the device operate in the safety operating zone (SOA) as defined by the Design Rule Check of the D01GH process. However, the LNA should not stay for a long time in this biasing situation that corresponds to an RF signal aggression situation. More studies will be developed to test the endurance of the LNA_{#A-HL} operating in this critical SOA zone. Concerning the second LNA design (LNA_{#R}), it keeps in the middle trend between these two situations of biasing for LNA_{#A}.

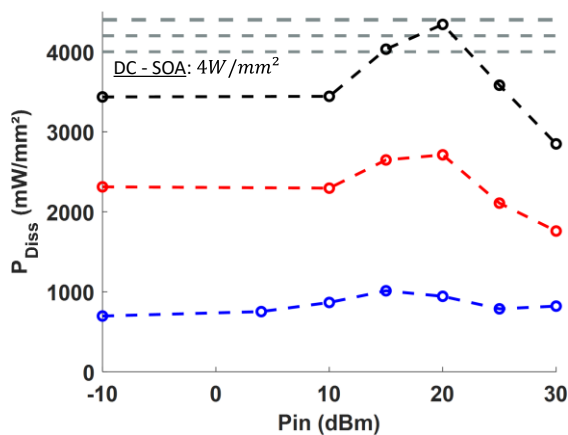


Figure 15: Dissipated power, defined as $P_{DC-natural} - (P_{out-natural} - P_{in-natural})$ versus $P_{in}(dBm)$ for LNA_{#A-LN}, LNA_{#A-HL} and LNA_{#R}.

Conclusions

Three RF step-stress tests sequences have been proposed for three single-stage MMIC GaN X-band LNAs. The proposed GaN LNA is reconfigurable when the input power level increases, as a protection strategy. Thus this LNA can endure overdrive RF signals up to 30 dBm, still keeping its electrical and noise parameters operational. This agile LNA has been compared to robust design LNA using larger device. The best noise figure is achieved with our reconfigurable LNA in “low-noise” biasing configuration, while a 9 dB improvement can be measured on the input power level at 1dB compression point when tuning to “high linearity” mode. However, the best linearity is still achieved for the robust LNA design, in spite of slightly degraded noise figure. RF step stresses are applied to each design strategies, and a weak degradation is obtained for the two LNAs operating in high linearity mode (agile LNA and robust LNA). By keeping the agile LNA under its low noise mode, the amplifier degrades significantly on its electrical and noise parameters. This work opens the way to an alternative of

traditional receivers that need a limiter between the antenna and the LNA (at the price of degraded noise performances with this later approach). From [S] parameters and NF_{50} measurements, our strategy to (self)reconfigure the agile LNA_{#A} from LNA_{#A-LN} to LNA_{#A-HL} according to the incident jamming input power level is proven, as this later configuration keeps the [S] parameters as well as the NF_{50} measurement stable after RF stress level up to 30 dBm. The three versions of the LNAs are destroyed for RF levels between 30 and 35 dBm. A study of the leakage current as a function of the input power shows that the final destruction occurs when the leakage current reaches the same 10mA limit at RF signal level of 30dBm (35 dBm for destruction)

Acknowledgement

This work was supported by the LAAS-CNRS PROOF platform, partly financed by the Occitanie region.

References

- [1] M. Rudolph *et al.*, « Analysis of the Survivability of GaN Low-Noise Amplifiers », *IEEE Trans. Microwave Theory Techn.*, vol. 55, n° 1, p. 37-43, janv. 2007, doi: 10.1109/TMTT.2006.886907.
- [2] M. Rudolph *et al.*, « Highly robust X-band LNA with extremely short recovery time », in *2009 IEEE MTT-S International Microwave Symposium Digest*, Boston, MA, USA: IEEE, juin 2009, p. 781-784. doi: 10.1109/MWSYM.2009.5165813.
- [3] A. Liero, M. Dewitz, S. kuhn, N. Chaturvedi, J. Xu, et M. Rudolph, « On the Recovery Time of Highly Robust Low-Noise Amplifiers », *IEEE Trans. Microwave Theory Techn.*, vol. 58, n° 4, p. 781-787, avr. 2010, doi: 10.1109/TMTT.2010.2041519.
- [4] A. Bettidi, F. Corsaro, A. Cetronio, A. Nanni, M. Peroni, et P. Romanini, « X-band GaN-HEMT LNA performance versus robustness trade-off », in *2009 European Microwave Conference (EuMC)*, sept. 2009, p. 1792-1795. doi:10.23919/EUMC.2009.5296145.
- [5] B. Pinault, J.G. Tartarin, D. Saugnon, R. Leblanc « A new method for designing robust low noise amplifier », in *ESA-ESTEC 1st space microwave conference proceedings*, may 2023, Noordwijk, The Netherlands, 6p.